M&C 2001 Salt Lake City, Utah, USA, September 2001.

ADDITIVE ANGULAR DEPENDENT REBALANCE ACCELERATION OF THE DISCRETE ORDINATES TRANSPORT CALCULATIONS

Chang Je Park and Nam Zin Cho
Korea Advanced Institute of Science and Technology
Department of Nuclear Engineering
373-1 Kusong-dong, Yusong-gu
Taejon, Korea 305-701
Email : nzcho@mail.kaist.ac.kr

Keywords : Additive angular dependent rebalance (AADR) acceleration, linear multiple balance (LMB) scheme, Fourier analysis, spectral radius

ABSTRACT

In solving the discrete ordinates neutron transport equation, the additive angular dependent rebalance (AADR) acceleration method proposed by the authors previously is simple to implement, unconditionally stable and very effective. For slab geometry problems, it is demonstrated via Fourier analysis that the spectral radius of the AADR acceleration in S_4-like and DP_1-like rebalances as well as DP_0-like rebalance is less than that of diffusion synthetic acceleration (DSA). This AADR acceleration method is easily extendable to DP_N-like and low-order S_N-like rebalancing and it does not require consistent discretizations between the high-order and low-order equations as does DSA. The continuous Fourier analysis is also performed for rectangular geometry to analyze the stability of the AADR acceleration method. This Fourier analysis shows that the AADR with directional S_2-like weighting functions which uses two different rebalance factors for x and y directions per octant provide better results than the AADR with the normal S_2-like weighting functions which uses a single weighting function per octant. The low-order equation in AADR is solved by a preconditioned Bi-CGSTAB algorithm, which reduces computational burden significantly.

1. INTRODUCTION

Various algorithms have been developed in the past to accelerate the source iteration for discrete ordinates equation. Among these algorithms, the diffusion synthetic acceleration (DSA) (Alcouffe, 1977, Larsen, 1982) is most popular and unconditionally stable and rapidly convergent. But it needs consistency of discretization schemes between high-order equation and low-order equation. To escape those burdens, various methods have been suggested and tested. Recently boundary projection acceleration (BPA) (Adams and Martin, 1988), transport synthetic acceleration (TSA) (Ramone and Adams, 1997), and angular dependent rebalance (ADR) (Hong and Cho, 1997, Hong and Cho, 1998) acceleration methods were developed. Unlike DSA, these schemes have generality with respect to geometry, discretization scheme, and mesh shape.

We have developed an additive angular dependent rebalance (AADR) algorithm (Park and Cho, 2000, Cho and Park, 2001) which is a linearized form of angular dependent rebalance

(ADR) acceleration method. It was found that the effect of acceleration depends on the weighting function and optimal rebalance factor could be obtained from a continuous Fourier analysis in slab geometry. Among various weighting functions, a linear weighting function ($W_n = |\mu_n| + 2.27$) gives spectral radius less than $0.1865c$, which is smaller than $0.2247c$ of DSA.

In two-dimensional problems, the formula of AADR becomes more complicated and considers more rebalance factors to get better convergence. The optimal weighting function may also be chosen via standard Fourier analysis which was done in slab geometry. We find that the S_2-like acceleration of AADR does not give any merits compared with existing DSA method but a directional rebalance factor gives better results. This result is similar to that of the DP_1-like or S_4-like acceleration of AADR in slab geometry. That is, the use of more rebalance factors requires fewer iterations but it might take slightly longer computing time to solve the low-order equation. To solve the low-order equation effectively, a preconditioned Bi-CGSTAB algorithm is used. The preconditioner is obtained by a "transport sweep" incomplete factorization in this study.

In Section 2, we briefly describe the differencing schemes which are considered in this paper. The diamond difference (DD) and the linear multiple balance (LMB) schemes (Park and Cho, 2001) are briefly described for rectangular geometry. In the linear multiple balance approach, one mesh cell is divided into two subcells with quadratic approximation for the angular flux distribution. Several multiple balance equations are used to relate center angular flux with average angular flux by Simpson's rule. From the analysis of spatial truncation error, the accuracy of the linear multiple balance scheme is better than that of diamond difference scheme. The positivity of the method is also stronger than that of diamond differencing. In Section 3, we analyze the additive angular rebalance (AADR) acceleration with continuous Fourier analysis. In Section 4, we give the numerical results, and finally in Section 5, we present the conclusions.

2. DERIVATION OF SEVERAL DISCRETIZATION SCHEMES

To apply AADR, we consider several different discretizing schemes - diamond difference (DD) scheme, linear multiple balance (LMB) scheme, and nodal schemes (C-C and C-L). Only DD and LMB schemes are described in this paper for rectangular geometry and the derivations of nodal schemes are easily found (Khalil, 1985). One group x-y geometry discrete ordinates transport equation is

$$\mu_n \frac{d\psi_n(x,y)}{dx} + \eta_n \frac{d\psi_n(x,y)}{dy} + \sigma\psi_n(x,y) = q_n(x,y), \tag{1}$$

where

$$\begin{aligned} q_n(x,y) &= \sigma_s\phi(x,y) + S_n(x,y), \\ \phi(x,y) &= \sum_{n=1}^{N} w_n\psi_n(x,y), \end{aligned} \tag{2}$$

and μ_n, η_n and w_n are a discrete ordinate set and its weight, respectively. Integrating over $x_{i-1/2} < x < x_{i+1/2}$ and $y_{j-1/2} < y < y_{j+1/2}$, we obtain the spatial balance equation as

$$\frac{\mu_n}{\Delta_i}(\psi_{n,i+1/2,j} - \psi_{n,i-1/2,j}) + \frac{\eta_n}{\Delta_j}(\psi_{n,i,j+1/2} - \psi_{n,i,j-1/2}) + \sigma\psi_{n,i,j} = q_{n,i,j}, \tag{3}$$

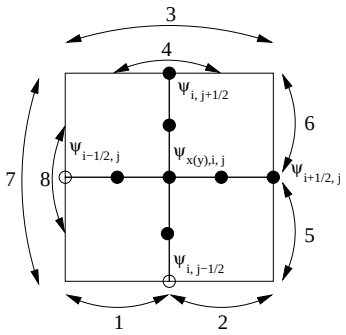

Figure 1: Configuration of unknowns of two dimensional problem.

where

$$\begin{aligned}
\psi_{n,i+1/2,j} &= \frac{1}{\Delta_j}\int_{y_{j-1/2}}^{y_{j+1/2}} \psi_n(x_{i+1/2},y)dy,\\
\psi_{n,i,j+1/2} &= \frac{1}{\Delta_i}\int_{x_{i-1/2}}^{x_{i+1/2}} \psi_n(x,y_{j+1/2})dx,\\
\psi_{n,i,j} &= \frac{1}{\Delta_i\Delta_j}\int_{x_{i-1/2}}^{x_{i+1/2}}\int_{y_{j-1/2}}^{y_{j+1/2}} \psi_n(x,y)dxdy,\\
q_{n,i,j} &= \frac{1}{\Delta_i\Delta_j}\int_{x_{i-1/2}}^{x_{i+1/2}}\int_{y_{j-1/2}}^{y_{j+1/2}} q_n(x,y)dxdy,\\
\Delta_i &= x_{i+1/2}-x_{i-1/2},\ \Delta_j = y_{j+1/2}-y_{j-1/2}.
\end{aligned} \tag{4}$$

Diamond difference (DD) approximation is

$$\begin{aligned}
\psi_{n,i,j} &= \frac{1}{2}(\psi_{n,i+1/2,j}+\psi_{n,i-1/2,j}),\\
\psi_{n,i,j} &= \frac{1}{2}(\psi_{n,i,j+1/2}+\psi_{n,i,j-1/2}).
\end{aligned} \tag{5}$$

Thus we can obtain the average angular flux by inserting Eq. (5) into Eq. (3).

Linear multiple balance (LMB) scheme uses eight multiple balance equations on a mesh cell divided into four subcells in rectangular geometry. For example, the unknowns of linear multiple balance (LMB) equations are given in a cell in Fig. 1. Especially, two balance equations (balance 4 and 8) are set up to overlap over the subcells. This is in contrast to the nonlinear corner balance scheme(Castrianni and Adams, 1998).

The first four linear multiple balance equations for x-direction are given by

$$\begin{aligned}
&2\frac{\mu_n}{\Delta_i}(\psi_{nx,i,j}-\psi_{n,i-1/2,j})+\frac{\eta_n}{\Delta_j}(\psi_{n,i,j+1/2}-\psi_{n,i,j-1/2})+\sigma\frac{\psi_{n,i-1/2,j}+4\psi_{n,i-1/4,j}+\psi_{nx,i,j}}{6}=q^L_{n,x,i,j},\\
&2\frac{\mu_n}{\Delta_i}(\psi_{n,i+1/2,j}-\psi_{nx,i,j})+\frac{\eta_n}{\Delta_j}(\psi_{n,i,j+1/2}-\psi_{n,i,j-1/2})+\sigma\frac{\psi_{nx,i,j}+4\psi_{n,i+1/4,j}+\psi_{n,i+1/2,j}}{6}=q^R_{n,x,i,j},\\
&\frac{\mu_n}{\Delta_i}(\psi_{n,i+1/2,j}-\psi_{n,i-1/2,j})+\frac{\eta_n}{\Delta_j}(\psi_{n,i,j+1/2}-\psi_{n,i,j-1/2})+\sigma\frac{\psi_{n,i-1/2,j}+4\psi_{nx,i,j}+\psi_{n,i+1/2,j}}{6}=q^L_{n,x,i,j}+q^R_{n,x,i,j},\\
&2\frac{\mu_n}{\Delta_i}(\psi_{n,i+1/4,j}-\psi_{n,i-1/4,j})+\frac{\eta_n}{\Delta_j}(\psi_{n,i,j+1/2}-\psi_{n,i,j-1/2})+\sigma\frac{\psi_{n,i-1/4,j}+4\psi_{nx,i,j}+\psi_{n,i+1/4,j}}{6}=\frac{q^L_{n,x,i,j}+q^R_{n,x,i,j}}{2},
\end{aligned} \tag{6}$$

where

$$\begin{aligned}
\psi_{nx,i,j} &= \frac{1}{\Delta_j}\int_{y_{j-1/2}}^{y_{j+1/2}} \psi_n(x_i,y)dx, \\
q^R_{n,x,i,j} &= \frac{2}{\Delta_i\Delta_j}\int_{x_i}^{x_{i+1/2}}\int_{y_{j-1/2}}^{y_{j+1/2}} q_n(x,y)dxdy, \\
q^L_{n,x,i,j} &= \frac{2}{\Delta_i\Delta_j}\int_{x_{i-1/2}}^{x_i}\int_{y_{j-1/2}}^{y_{j+1/2}} q_n(x,y)dxdy.
\end{aligned} \tag{7}$$

The other four linear multiple balance equations for y-direction are also derived similarly. An average angular flux can be obtained from the neutron balance equation:

$$\psi_{n,i,j} = \frac{1}{\sigma}\{q_{n,i,j} - \frac{\mu_n}{\Delta_i}(\psi_{n,i+1/2,j} - \psi_{n,i-1/2,j}) - \frac{\eta_n}{\Delta_j}(\psi_{n,i,j+1/2} - \psi_{n,i,j-1/2})\}. \tag{8}$$

3. FOURIER ANALYSIS FOR AADR ACCELERATION

3.1 Slab Geometry

The standard source iteration (SI) of the discrete ordinates equation for slab geometry is given by

$$\begin{aligned}
&\mu\frac{d}{dx}\psi^{l+1/2} + \sigma\psi^{l+1/2} = \sigma_s\phi^l + Q, \\
&\phi^{l+1} = \frac{1}{2}\int_{-1}^{1}\psi^{l+1/2}d\mu = \phi^{l+1/2},
\end{aligned} \tag{9}$$

where l is the iteration index. It is well known that the spectral radius (ρ) of SI is the scattering ratio($c = \sigma_s/\sigma$). If c goes to unity, the convergence becomes worse and it might well need many iterations and long computing time. For this reason, many acceleration methods are suggested and developed. Among them, the most popular diffusion synthetic acceleration (DSA) is given as

$$\begin{aligned}
&\mu\frac{d}{dx}\psi^{l+1/2} + \sigma\psi^{l+1/2} = \sigma_s\phi^l + Q, \\
&\phi_0^{l+1/2} = \frac{1}{2}\int_{-1}^{1}\psi^{l+1/2}d\mu, \\
&-\frac{d}{dx}\frac{1}{3\sigma}\frac{d}{dx}f^{l+1} + \sigma f^{l+1} = \sigma_s(\phi^{l+1} - \phi^l),
\end{aligned} \tag{10}$$

and

$$\phi^{l+1} = \phi^{l+1/2} + f^{l+1}. \tag{11}$$

The spectral radius of DSA is less than $0.2247c$, whose unconditional stability enjoys its wide use to accelerate the transport solution. But it needs the consistency of discretization schemes between the low-order and the high-order equations. Therefore, it is difficult to derive the DSA equation for nonlinear discretization schemes as well as multiple balance schemes. To overcome this constraint of DSA, rebalance methods (could also be called synthetic methods)

have been suggested since late 1980's. It solves a low-order equation which is a similar form to the high-order equation. These methods include boundary projection acceleration (BPA), transport synthetic acceleration (TSA), and angular dependent rebalance (ADR) acceleration methods. The additive angular dependent rebalance (AADR) method is a linearized form of ADR. First, the AADR acceleration method is applied to slab geometry with DP_N-like and S_N-like rebalance factors. In the case of DP_N-like weighted AADR method, the rebalance factors (f) are defined as

$$\sum_{n=0}^{N} f_{n,\pm} P_n(2\mu \mp 1) = \psi^{l+1} - \psi^{l+1/2}, \quad \mu \gtrless 0, \tag{12}$$

where P_n is an n-th order Legendre polynomial. It uses $2(N+1)$ different rebalance factors, and needs $(N+1)$ different weighting functions to be introduced later. In contrast, the rebalance factors in the low order S_N-like weighted AADR method are defined as

$$\begin{aligned} f_{k,+}^{l+1} &= \psi^{l+1} - \psi^{l+1/2}, \quad \mu > 0, \\ f_{k,-}^{l+1} &= \psi^{l+1} - \psi^{l+1/2}, \quad \mu < 0, \quad k = 0, \cdots, (N-2)/2. \end{aligned} \tag{13}$$

It uses N rebalance factors, but needs only one weighting function to determine rebalance factors. We note that the DP_0-like weighted and S_2-like weighted AADR methods are equivalent. To derive AADR in DP_0-like (or S_2-like) form, we begin with the following transport equation with isotropic scattering:

$$\begin{aligned} \mu \frac{d}{dx}\psi^{l+1/2} + \sigma\psi^{l+1/2} &= \sigma_s \phi^l + Q, \\ \phi^{l+1/2} &= \frac{1}{2}\int_{-1}^{1} \psi^{l+1/2} d\mu. \end{aligned} \tag{14}$$

The low-order equation for acceleration is derived by changing all the indices in the above equation to $l+1$, from which Eq.(14) is then subtracted. We integrate the resulting equation over half-angular space with a weighting function to obtain

$$\begin{aligned} k_1 \frac{d}{dx} f_+^{l+1} + k_0 \sigma f_+^{l+1} &= k_0 \sigma_s (\phi^{l+1} - \phi^l), \quad \mu > 0, \\ -k_1 \frac{d}{dx} f_-^{l+1} + k_0 \sigma f_-^{l+1} &= k_0 \sigma_s (\phi^{l+1} - \phi^l), \quad \mu < 0, \\ \phi^{l+1} &= \phi^{l+1/2} + \frac{f_+^{l+1} + f_-^{l+1}}{2}, \end{aligned} \tag{15}$$

where

$$\begin{aligned} f_+^{l+1} &= \psi^{l+1} - \psi^{l+1/2}, \quad \mu > 0, \\ f_-^{l+1} &= \psi^{l+1} - \psi^{l+1/2}, \quad \mu < 0, \\ k_0 = \int_0^1 W(\mu) d\mu, &\quad k_1 = \int_0^1 W(\mu)\mu d\mu, \end{aligned} \tag{16}$$

and $W(\mu)$ is a weighting function to be chosen later so that the Fourier analysis indicates the smallest spectral radius (optimal weighting function). As mentioned, the AADR method

is easily extendable to DP_N-like and low-order S_N-like rebalancing. So we also analyze the AADR with DP_1-like form, of which rebalance equations are given below.

$$\begin{aligned}
k_{01}\frac{d}{dx}f_{0,+}^{l+1}+(2k_{02}+k_{01})\frac{d}{dx}f_{1,+}^{l+1}+\sigma(f_{0,+}^{l+1}+(2k_{01}+1)f_{1,+}^{l+1})&=\sigma_s(\phi^{l+1}-\phi^l), \quad \mu>0,\\
k_{11}\frac{d}{dx}f_{0,+}^{l+1}+(2k_{12}+k_{11})\frac{d}{dx}f_{1,+}^{l+1}+\sigma(f_{0,+}^{l+1}+(2k_{11}+1)f_{1,+}^{l+1})&=\sigma_s(\phi^{l+1}-\phi^l), \quad \mu>0,\\
-k_{01}\frac{d}{dx}f_{0,-}^{l+1}+(2k_{02}+k_{01})\frac{d}{dx}f_{1,-}^{l+1}+\sigma(f_{0,-}^{l+1}-(2k_{01}+1)f_{1,-}^{l+1})&=\sigma_s(\phi^{l+1}-\phi^l), \quad \mu<0,\\
-k_{11}\frac{d}{dx}f_{0,-}^{l+1}+(2k_{12}+k_{11})\frac{d}{dx}f_{1,-}^{l+1}+\sigma(f_{0,-}^{l+1}-(2k_{11}+1)f_{1,-}^{l+1})&=\sigma_s(\phi^{l+1}-\phi^l), \quad \mu<0,
\end{aligned} \tag{17}$$

where

$$\begin{aligned}
&\sum_{n=0}^{1}f_{n,+}^{l+1}P_n(2\mu-1)=\psi^{l+1}-\psi^{l+1/2}, \quad \mu>0,\\
&\sum_{n=0}^{1}f_{n,-}^{l+1}P_n(2\mu+1)=\psi^{l+1}-\psi^{l+1/2}, \quad \mu<0,\\
&k_{m1}=\Big(\int_0^1\mu W_m(\mu)d\mu\Big)\Big/\Big(\int_0^1 W_m(\mu)d\mu\Big),\\
&k_{m2}=\Big(\int_0^1\mu^2 W_m(\mu)d\mu\Big)\Big/\Big(\int_0^1 W_m(\mu)d\mu\Big), \quad m=0,1.
\end{aligned} \tag{18}$$

Another form of AADR uses the S_4-like rebalance factors, which is easily determined compared with DP_1-like form and needs only a single weighting function. The rebalance equations of AADR in S_4-like form are given as

$$\begin{aligned}
l_0\frac{d}{dx}f_{0,+}^{l+1}+\sigma f_{0,+}^{l+1}&=\sigma_s(\phi^{l+1}-\phi^l), \quad \mu>0,\\
l_1\frac{d}{dx}f_{1,+}^{l+1}+\sigma f_{1,+}^{l+1}&=\sigma_s(\phi^{l+1}-\phi^l), \quad \mu>0,\\
-l_0\frac{d}{dx}f_{0,-}^{l+1}+\sigma f_{0,-}^{l+1}&=\sigma_s(\phi^{l+1}-\phi^l), \quad \mu<0,\\
-l_1\frac{d}{dx}f_{1,-}^{l+1}+\sigma f_{1,-}^{l+1}&=\sigma_s(\phi^{l+1}-\phi^l), \quad \mu<0,
\end{aligned} \tag{19}$$

where

$$\begin{aligned}
f_{0,+}^{l+1}&=\psi^{l+1}-\psi^{l+1/2}, \quad 0<\mu<1/\sqrt{2},\\
f_{1,+}^{l+1}&=\psi^{l+1}-\psi^{l+1/2}, \quad 1/\sqrt{2}<\mu<1,\\
f_{0,-}^{l+1}&=\psi^{l+1}-\psi^{l+1/2}, \quad -1/\sqrt{2}<\mu<0,\\
f_{1,-}^{l+1}&=\psi^{l+1}-\psi^{l+1/2}, \quad -1<\mu<-1/\sqrt{2},\\
l_0&=\Big(\int_0^{1/\sqrt{2}}\mu W(\mu)d\mu\Big)\Big/\Big(\int_0^{1/\sqrt{2}}W(\mu)d\mu\Big),\\
l_1&=\Big(\int_{1/\sqrt{2}}^{1}\mu W(\mu)d\mu\Big)\Big/\Big(\int_{1/\sqrt{2}}^{1}W(\mu)d\mu\Big).
\end{aligned} \tag{20}$$

In summary, we get a general form of the spectral radius with weighting parameter $a(\lambda)$ using the standard Fourier analysis:

$$\rho \le \sup_\lambda \; c \left| \frac{1}{2} \int_{-1}^{1} \frac{1 - \frac{a(\lambda)}{1-a(\lambda)} \lambda^2 \mu^2}{1 + \lambda^2 \mu^2} d\mu \right| = \sup_\lambda \; c \left| \frac{\lambda a(\lambda) - \arctan(\lambda)}{(a(\lambda) - 1)\lambda} \right|. \tag{21}$$

Depending on the weighting parameter $a(\lambda)$, we can classify several acceleration methods as

$$\begin{aligned}
&\text{(i) SI :} && a(\lambda) = 0, \quad \rho = c, \\
&\text{(ii) DSA :} && a(\lambda) = \frac{1}{1 + \frac{\lambda^2}{3}}, \quad \rho < 0.2247c, \\
&\text{(iii) AADR(DP}_0\text{) :} && a(\lambda) = \frac{1}{1 + (\frac{k_1}{k_0}\lambda)^2}, \quad \rho < 0.1865c, \\
&\text{(iv) AADR(DP}_1\text{) :} && a(\lambda) = A/B, \quad \rho < 0.0553c, \\
&\text{(v) AADR(S}_4\text{) :} && a(\lambda) = \frac{1}{2}\Big(\frac{1}{1 + (l_0\lambda)^2} + \frac{1}{1 + (l_1\lambda)^2} \Big), \quad \rho < 0.0485c,
\end{aligned} \tag{22}$$

where

$$\begin{aligned}
A &= 2(k_{00} - k_{10})^2 + (k_{01}(2k_{01} + k_{10} + 2k_{10}^2 - k_{00}(1 + 2k_{10}) \\
&\quad + (k_{00} + 2k_{00}^2 - 4k_{01} - 2k_{00}k_{10})k_{11} + 2k_{11}^2)\lambda^2, \\
B &= 2\Big((k_{00} - k_{10} - (k_{01}k_{10} - k_{00}k_{11})\lambda^2)^2 + (k_{01} - k_{11})^2\lambda^4 \Big).
\end{aligned} \tag{23}$$

For (iii), (iv), and (v) above, optimal weighting functions $W(\mu)$ are chosen such that $a(\lambda)$ leads to the smallest spectral radius through k's and l's. The AADR method with S_4-like rebalance factors gives the smallest spectral radius, but it may take longer computing time than S_2-like weighted AADR method due to the increased number of rebalance factors in the low-order equation.

3.2 Rectangular Geometry

It is more complicated and needs more rebalance factors when we apply the AADR method to rectangular geometry problems. The AADR with the normal S_2-like rebalance form is written as

$$\begin{aligned}
&\mu_n \frac{\partial}{\partial x}\psi_n^{l+1/2} + \eta_n \frac{\partial}{\partial y}\psi_n^{l+1/2} + \sigma\psi_n^{l+1/2} = \sigma_s\phi^l + S_n, \\
&\phi^{l+1/2} = \frac{1}{4}\sum_n w_n \psi_n^{l+1/2}, \\
&k_1 \frac{\partial}{\partial x} f_1^{l+1} + k_2 \frac{\partial}{\partial y} f_1^{l+1} + \sigma f_1^{l+1} = \sigma_s(\phi^{l+1} - \phi^l), \quad \mu_n > 0,\ \eta_n > 0, \\
&-k_1 \frac{\partial}{\partial x} f_2^{l+1} + k_2 \frac{\partial}{\partial y} f_2^{l+1} + \sigma f_2^{l+1} = \sigma_s(\phi^{l+1} - \phi^l), \quad \mu_n < 0,\ \eta_n > 0, \\
&-k_1 \frac{\partial}{\partial x} f_3^{l+1} - k_2 \frac{\partial}{\partial y} f_3^{l+1} + \sigma f_3^{l+1} = \sigma_s(\phi^{l+1} - \phi^l), \quad \mu_n < 0,\ \eta_n < 0, \\
&k_1 \frac{\partial}{\partial x} f_4^{l+1} - k_2 \frac{\partial}{\partial y} f_4^{l+1} + \sigma f_4^{l+1} = \sigma_s(\phi^{l+1} - \phi^l), \quad \mu_n > 0,\ \eta_n < 0, \\
&\phi^{l+1} = \phi^{l+1/2} + \frac{f_1^{l+1} + f_2^{l+1} + f_3^{l+1} + f_4^{l+1}}{4},
\end{aligned} \tag{24}$$

where

$$
\begin{aligned}
k_1 &= \frac{\sum_n w_n \mu_n W(\mu_n, \eta_n)}{\sum_n w_n W(\mu_n, \eta_n)}, \\
k_2 &= \frac{\sum_n w_n \eta_n W(\mu_n, \eta_n)}{\sum_n w_n W(\mu_n, \eta_n)}, \\
f_1 &= \psi_n^{l+1} - \psi_n^{l+1/2}, \quad \mu_n > 0, \ \eta_n > 0, \\
f_2 &= \psi_n^{l+1} - \psi_n^{l+1/2}, \quad \mu_n < 0, \ \eta_n > 0, \\
f_3 &= \psi_n^{l+1} - \psi_n^{l+1/2}, \quad \mu_n < 0, \ \eta_n < 0, \\
f_4 &= \psi_n^{l+1} - \psi_n^{l+1/2}, \quad \mu_n > 0, \ \eta_n < 0.
\end{aligned} \tag{25}
$$

To get the optimal spectral radius, weighting coefficients (k_1, k_2) are obtained from Fourier analysis. Weighting functions are also evaluated to satisfy this weighting coefficients. First, we suggest a linear type of weighting function such as

$$
\begin{aligned}
&k_1 = k_2 = 0.7, \quad \rho < 0.4469c, \\
&W(\mu, \eta) = |\mu| + |\eta| - 0.5.
\end{aligned} \tag{26}
$$

The results do not provide good enough spectral radii compared with those of DSA ($\rho < 0.2247c$). Thus we next suggest directional weighting functions for AADR, where different directional rebalance factors are used to update different directional scalar fluxes. The rebalance equations of AADR with directional rebalance factors are given as

$$
\begin{aligned}
k_u \frac{\partial}{\partial x} f_{1,u}^{l+1} + k_v \frac{\partial}{\partial y} f_{1,u}^{l+1} + \sigma f_{1,u}^{l+1} &= \sigma_s(\phi^{l+1} - \phi^l), \\
-k_u \frac{\partial}{\partial x} f_{2,u}^{l+1} + k_v \frac{\partial}{\partial y} f_{2,u}^{l+1} + \sigma f_{2,u}^{l+1} &= \sigma_s(\phi^{l+1} - \phi^l), \\
-k_u \frac{\partial}{\partial x} f_{3,u}^{l+1} - k_v \frac{\partial}{\partial y} f_{3,u}^{l+1} + \sigma f_{3,u}^{l+1} &= \sigma_s(\phi^{l+1} - \phi^l), \\
k_u \frac{\partial}{\partial x} f_{4,u}^{l+1} - k_v \frac{\partial}{\partial y} f_{4,u}^{l+1} + \sigma f_{4,u}^{l+1} &= \sigma_s(\phi^{l+1} - \phi^l), \\
u = x, v = y \text{ or } u = y, v = x,&
\end{aligned} \tag{27}
$$

where

$$
\begin{aligned}
f_{m,x} &= \psi_n^{l+1} - \psi_n^{l+1/2} \ \text{ if } \ W = W_x, \\
f_{m,y} &= \psi_n^{l+1} - \psi_n^{l+1/2} \ \text{ if } \ W = W_y, \quad m = 1, 2, 3, 4, \\
k_x &= \frac{\sum_n w_n \mu_n W_x(\mu_n, \eta_n)}{\sum_n w_n W_x(\mu_n, \eta_n)} = \frac{\sum_n w_n \eta_n W_y(\mu_n, \eta_n)}{\sum_n w_n W_y(\mu_n, \eta_n)}, \\
k_y &= \frac{\sum_n w_n \mu_n W_y(\mu_n, \eta_n)}{\sum_n w_n W_y(\mu_n, \eta_n)} = \frac{\sum_n w_n \eta_n W_x(\mu_n, \eta_n)}{\sum_n w_n W_x(\mu_n, \eta_n)}.
\end{aligned} \tag{28}
$$

To choose directional rebalance factors properly, several conditions are given for directional

weighting functions ($W_x,\ W_y$) such as

$$\begin{aligned}
&W_x + W_y = 2,\\
&\sum_n w_n W_x(\mu_n,\eta_n) = \sum_n w_n W_y(\mu_n,\eta_n) = 1,\\
&\sum_n w_n \mu_n W_x(\mu_n,\eta_n) = \sum_n w_n \eta_n W_y(\mu_n,\eta_n),\\
&\sum_n w_n \eta_n W_x(\mu_n,\eta_n) = \sum_n w_n \mu_n W_y(\mu_n,\eta_n),\\
&W_x(\mu_n,\eta_n) = a(|\mu_n| - |\eta_n|) + 1, \quad W_y(\mu_n,\eta_n) = -a(|\mu_n| - |\eta_n|) + 1,
\end{aligned} \tag{29}$$

where a is determined for $k_x,\ k_y$ which in turn are determined optimally from Fourier analysis. The scalar flux is updated as

$$\begin{aligned}
\phi^{l+1} - \phi^{l+1/2} &= \sum_n w_n(\psi_n^{l+1} - \psi_n^{l+1/2}),\\
&= \frac{1}{4}\sum_n w_n \frac{W_x + W_y}{2}(\psi_n^{l+1} - \psi_n^{l+1/2}),\\
&= \frac{1}{4}\sum_n w_n \left\{ \frac{W_x}{2}(\psi_n^{l+1} - \psi_n^{l+1/2}) + \frac{W_y}{2}(\psi_n^{l+1} - \psi_n^{l+1/2}) \right\},\\
&= \frac{1}{4}\sum_n w_n \left\{ \frac{W_x}{2} f_{m,x}^{l+1} + \frac{W_y}{2} f_{m,y}^{l+1} \right\},\\
&= \frac{f_{m,x} + f_{m,y}}{8}, \quad m = 1,2,3,4.
\end{aligned} \tag{30}$$

To get the optimal spectral radius, weighting coefficients (k_x, k_y) are obtained. The optimal weighting functions are also evaluated to satisfy these weighting coefficients:

$$k_x = 0.8,\ k_y = 0.2, \quad W_x = 2.4(|\mu_n| - |\eta_n|) + 1,\ W_y = -2.4(|\mu_n| - |\eta_n|) + 1, \quad \rho < 0.1275c. \tag{31}$$

We find that the directional weighting functions provide better convergence than the normal S_2-like weighting in AADR.

In the same way as in slab geometry, the spectral radius (ρ) is expressed in a general form using Fourier analysis as

$$\rho = sup_{\lambda_x,\lambda_y} \left| \frac{c}{4} \sum_n w_n \frac{1 - K(\lambda_x,\lambda_y)(\mu_n\lambda_x + \eta_n\lambda_y)^2}{1 + (\mu_n\lambda_x + \eta_n\lambda_y)^2} \right|, \tag{32}$$

where $K(\lambda_x,\lambda_y)$ represents a weighting parameter and it is given in different form depending on the acceleration methods:

$$\begin{aligned}
&\text{(i) SI}: \quad K(\lambda_x,\lambda_y) = 0,\\
&\text{(ii) DSA}: \quad K(\lambda_x,\lambda_y) = \frac{1}{\lambda_x^2/3 + \lambda_y^2/3},\\
&\text{(iii) AADR(n)}: \quad K(\lambda_x,\lambda_y) = \frac{1 + (k_1\lambda_x)^2 + (k_2\lambda_y)^2}{(k_1\lambda_x)^2 + (k_2\lambda_y)^2 + ((k_1\lambda_x)^2 - (k_2\lambda_y)^2)^2},\\
&\text{(iv) AADR(d)}: \quad K(\lambda_x,\lambda_y) = \frac{1}{2}\frac{B(C + 2D - 1) + D(A + 2B - 1)}{(A + 2B - 1)(C + D - 1) + (C + 2D - 1)(A + B - 1)},
\end{aligned} \tag{33}$$

where

$$\begin{aligned} A &= ((k_x\lambda_x)^2 - (k_y\lambda_y)^2)^2, \quad B = 1 + (k_x\lambda_x)^2 + (k_y\lambda_y)^2, \\ C &= ((k_y\lambda_x)^2 - (k_x\lambda_y)^2)^2, \quad D = 1 + (k_y\lambda_x)^2 + (k_x\lambda_y)^2. \end{aligned} \tag{34}$$

The spectral radii of various methods are then given as

$$\begin{aligned} &\text{(i) SI :} \quad \rho = c, \\ &\text{(ii) DSA :} \quad \rho < 0.2247c, \\ &\text{(iii) AADR(n) : } \rho < 0.4469c \text{ (when } k_1 = k_2 = 0.7), \\ &\text{(iv) AADR(d) : } \rho < 0.1275c \text{ (when } k_x = 0.8,\ k_y = 0.2). \end{aligned} \tag{35}$$

Here, AADR(n) denotes AADR with the normal S_2-like rebalance factors and AADR(d) denotes AADR with the directional S_2-like rebalance factors. The spectral radius of AADR(d) is much less than those of AADR(n) and DSA. Considering directional rebalance factors, AADR(d) may need slightly longer computing time for the low-order equation than AADR(n) but it is compensated by fast convergence with reduced spectral radius.

3.3 Preconditioned Bi-CGSTAB Algorithm

The preconditioned Bi-CGSTAB algorithm used also reduces computational burden in AADR. The Bi-CGSTAB method is a variation of the conjugate gradient square (CGS) method which was developed to remedy the substantial buildup of rounding errors or possibly even overflow of the CGS method in cases of irregular convergence and it does not require a transpose of the operator. A preconditioned matrix $\mathbf{B}$ is determined in the following "transport sweep" incomplete factorization. For general cases, the low-order operator ($\mathbf{T}$) is defined as (Hong and Cho, 1998):

$$\begin{aligned} \mathbf{T}\vec{x} &= (\mathbf{I} - \mathbf{M})\vec{x}, \\ \mathbf{M}\vec{x} &= \sum_{\gamma=1}^{4} \vec{x}_\gamma, \end{aligned} \tag{36}$$

and

$$\vec{x}_\gamma = \mathbf{G}_\gamma^{-1}\vec{x}, \quad \gamma = 1, 2, 3, 4, \tag{37}$$

where $\mathbf{G}_\gamma$ is the transport sweep operator in octant γ.

Thus, we get an expression for $\mathbf{T}$ as

$$\mathbf{T}\vec{x} = (\mathbf{I} - \mathbf{G}_1^{-1} - \mathbf{G}_2^{-1} - \mathbf{G}_3^{-1} - \mathbf{G}_4^{-1})\vec{x}. \tag{38}$$

As a preconditioner $\mathbf{B}$, we take an incomplete factorization matrix from $\mathbf{T}$:

$$\mathbf{B}\vec{x} = (\mathbf{I} - \mathbf{G}_1^{-1})(\mathbf{I} - \mathbf{G}_2^{-1})(\mathbf{I} - \mathbf{G}_3^{-1})(\mathbf{I} - \mathbf{G}_4^{-1})\vec{x}. \tag{39}$$

It can be solved in the same way as the standard LU decomposition:

$$\begin{aligned} (\mathbf{I} - \mathbf{G}_1^{-1})\vec{z} = \vec{y} \quad &\Rightarrow \quad (\mathbf{G}_1 - \mathbf{I})\vec{z} = \mathbf{G}_1\vec{y}, \\ (\mathbf{I} - \mathbf{G}_2^{-1})\vec{v} = \vec{z} \quad &\Rightarrow \quad (\mathbf{G}_2 - \mathbf{I})\vec{v} = \mathbf{G}_2\vec{z}, \\ (\mathbf{I} - \mathbf{G}_3^{-1})\vec{u} = \vec{v} \quad &\Rightarrow \quad (\mathbf{G}_3 - \mathbf{I})\vec{u} = \mathbf{G}_3\vec{v}, \\ (\mathbf{I} - \mathbf{G}_4^{-1})\vec{x} = \vec{u} \quad &\Rightarrow \quad (\mathbf{G}_4 - \mathbf{I})\vec{x} = \mathbf{G}_4\vec{u}. \end{aligned} \tag{40}$$

4. NUMERICAL TESTS AND RESULTS

To assess performance of the additive angular dependent rebalance (AADR) acceleration, we tested it on several sample problems. The first test problem is an isotropic homogeneous slab, 50 cm wide with scattering ratio (c) of 1, a total cross section of 1 cm^{-1}. The vacuum boundary conditions are imposed on both sides and S_{16} Gauss-Legendre quadrature is used. Table I shows the number of iterations and computing times to converge the problem to a relative error of 10^{-9} using several weighting functions and cell widths. LMB and DD schemes are compared for several mesh sizes using AADR in DP_1 and S_4 forms as well as in DP_0 form. In comparing the computing times of the two discretization schemes, note that the orders of accuracy in LMB and DD are $O(\Delta^4)$ and $O(\Delta^2)$, respectively.

The second test problem is the McCoy-Larsen problem which is homogeneous and simple as shown in Fig. 2. It consists of a uniform, isotropically scattering with a scattering ratio(c) of 1. The problem is divided into 8×8 meshes and the total cross section σ is varied (i.e., $0.01 \leq \sigma \leq 6$). Table II shows the number of iterations and computing times. The criterion for average scalar flux is given 10^{-4} and S_8 quadrature is used. The results of AADR with single weighting function indicate that it needs more iterations and takes slightly longer computing time. But AADR with directional weighting functions is competitive with or outperform DSA, that are consistent with the results of Fourier analysis.

The third test is on the heterogeneous iron-water benchmark problem (Khalil, 1985). This problem is a diagonally symmetric, isotropic scattering $30cm \times 30cm$ rectangular box as shown in Fig. 3. Table III shows the material properties of iron-water benchmark problem. We solve it with S_8 angular quadrature set, 10×10 mesh division and a convergence criterion of 10^{-4}. The results for AADR and DSA methods are given in Table IV. Unfortunately, the DSA method in DANTSYS does not converge, which may have resulted from negativeness of the diamond difference scheme. So we compare the solutions of nodal methods (C-C, C-L) with those of LMB for AADR. To get the optimal convergence, weighting functions are selected as $W_x = 0.6(|\mu| - |\eta|) + 1$, $W_y = -0.6(|\mu| - |\eta|) + 1$. The computing time and number of iterations show that the LMB scheme with AADR provides good enough results.

5. CONCLUSIONS

We have described the additive angular dependent rebalance (AADR) method to accelerate the neutron transport equations in slab and rectangular geometries. The AADR with DP_1-like and S_4-like rebalance forms as well as with DP_0-like (or S_2-like) rebalance form uses physically based weighting functions with an optimal parameter leading to smaller spectral radii than that of DSA. From Fourier analysis in rectangular geometry, we find that the normal S_2-like weighted AADR method is not competitive with DSA method. But the directional S_2-like weighted AADR method gives good results from numerical tests as well as from Fourier analysis. We also find that AADR methods strongly depend on weighting functions and suitable weighting functions provide optimal convergence for the given problem. As a concluding remark, the additive angular dependent rebalance (AADR) acceleration method is useful and can offer various advantages over the existing methods.

ACKNOWLEDGEMENT

This work was supported in part by the Ministry of Science and Technology of Korea through the National Research Laboratory (NRL) Program.

REFERENCES

Adams, M. L. and Martin, W. R., 1988. Boundary Projection Acceleration : A New Approach to Synthetic Acceleration of Transport Calculations. *Nucl. Sci. Eng.* **100**, 177.

Alcouffe, R. E., 1977. Diffusion Synthetic Acceleration Methods for the Diamond-Differenced Discrete-Ordinates Equations. *Nucl. Sci. Eng.* **64**, 344.

Castrianni, C.L. and Adams, M.L., 1998. A Nonlinear Corner-Balance Spatial Discretization for Transport on Arbitrary Grids. *Nucl. Sci. Eng.*, **128**, 278.

Cho, N. Z. and Park, C. J., 2001. An Additive Angular Dependent Rebalance Acceleration Method for Neutron Transport Equations. to appear in *Trans. Am. Nucl. Soc.*, June.

Hong, S. G. and Cho, N. Z., 1997. A Rebalance Approach Nonlinear Iteration for Solving the Neutron Transport Equations. *Ann. of Nucl. Energy.* **24**, 146.

Hong, S. G. and Cho, N. Z., 1998. Angle-Dependent Rebalance Factor Method for Nodal Transport Problems in X-Y Geometry. *Trans. Am. Nucl. Soc.* **79**, 139.

Khalil, H., 1985. A Nodal Diffusion Technique for Synthetic Acceleration of Nodal S_N Calculations. *Nucl. Sci. Eng.* **90**, 263.

Larsen, E. W., 1982. Unconditionally Stable Diffusion Synthetic Acceleration Method for the Slab Geometry Discrete Ordinates Equations. PartI : Theory. *Nucl. Sci. Eng.* **82**, 47.

Lewis, E. E. and Miller, Jr. W. F. (1984) *Computational Methods of Neutron Transport*, John Wiley & Sons.

Park, C. J. and Cho, N. Z., 2001. A Linear Multiple Balance Method with High Accuracy for Discrete Ordinates Neutron Transport Equations. to appear in *Ann. of Nucl. Energy.*

Ramone, G. L. and Adams, M. L., 1997. A Transport Synthetic Acceleration Method for Transport Iterations. *Nucl. Sci. Eng.* **125**, 257.

Table I. Number of Iterations and Computing Times for LMB and DD

Method	$\sigma\Delta$	0.1	0.2	1.0	2.0
DSA	DD	13[c](0.25[d])	13(0.13)	12(0.04)	12(0.03)
AADR1 (DP_0 or S_2)	DD	12(0.45)	12(0.24)	12(0.06)	12(0.04)
$(\lvert\mu\rvert + 2.27)$[a]	LMB	12(0.97)	12(0.51)	12(0.13)	12(0.09)
AADR2 (S_4)	DD	7(0.51)	7(0.25)	7(0.06)	6(0.04)
$(P_2(\lvert\mu\rvert) - 1.5P_1(\lvert\mu\rvert) + 0.55)$[b]	LMB	7(1.06)	7(0.54)	6(0.10)	6(0.08)
AADR3 (DP_1)	DD	7(0.62)	7(0.31)	6(0.07)	6(0.04)
$(1,\ \lvert\mu\rvert)$					

[a] Weighting function,
[b] Legendre functions ($P_2(\mu) = \frac{1}{2}(3\mu^2 - 1),\ P_1(\mu) = \mu$),
[c] Number of iterations,
[d] Computing time (sec) on SUN-ULTRA1 system.

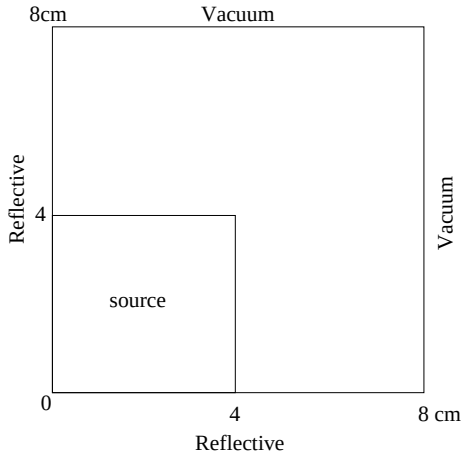

Figure 2: Configuration of 2D version of McCoy-Larsen problem.

Table II. Comparison of Number of Iterations and Computing Times[a] ($c = 1.0$)

σ	SI[b]		AADR(n)[c]		AADR(d)[d]		DSA[e]
	DD	LMB	DD	LMB	DD	LMB	DD
0.01	6[f]	6	4	5	4	4	4
	(0.06[g])	(0.09)	(0.08)	(0.19)	(0.10)	(0.12)	(0.99)
0.1	17	17	8	8	5	5	6
	(0.14)	(0.23)	(0.17)	(0.41)	(0.14)	(0.17)	(1.04)
1.0	269	236	8	8	6	6	5
	(1.88)	(2.91)	(0.28)	(0.41)	(0.27)	(0.33)	(1.01)
2.0	755	537	9	7	7	5	5
	(5.29)	(6.58)	(0.43)	(0.43)	(0.43)	(0.32)	(1.01)
4.0	2038	1083	10	6	7	6	8
	(15.71)	(13.40)	(0.65)	(0.38)	(0.51)	(0.37)	(1.08)
6.0	3473	1617	10	5	7	6	8
	(27.94)	(20.15)	(0.72)	(0.35)	(0.59)	(0.38)	(1.08)

[a]: SUN-ULTRA1, [b]: Source iteration,
[c]: AADR(n) with the normal S_2-like weighting function ($W = |\mu| + |\eta| - 0.5$),
[d]: AADR(d) with the directional S_2-like weighting functions
($W_x = 2.4(|\mu| - |\eta|) + 1,\ W_y = -2.4(|\mu| - |\eta|) + 1$),
[e]: DANTSYS code system,
[f]: Number of iterations, [g]: Computing time (sec).

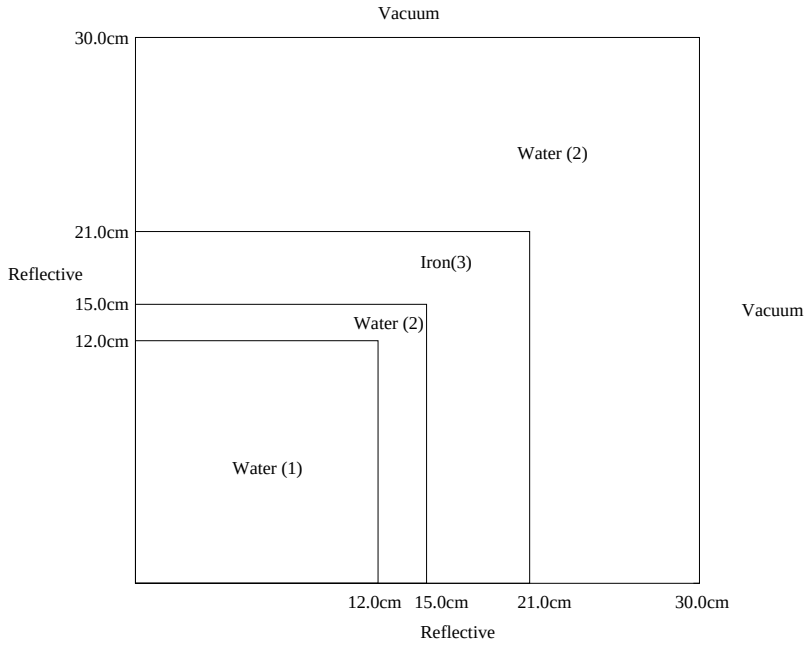

Figure 3: Configuration of the iron-water benchmark problem.

Table III. Material Properties for Iron-Water Benchmark Problem

Composition	$\sigma(cm^{-1})$	c	Source Strength
1(water)	3.33	0.994	1.0
2(water)	3.33	0.994	0.0
3(iron)	1.33	0.831	0.0

Table IV. Comparison of Number of Iterations and Computing Times

Method	Source Iteration			AADR(n)[a]			AADR(d)[b]			DSA[c]
Scheme	LMB	C-C[d]	C-L[e]	LMB	C-C	C-L	LMB	C-C	C-L	DD
Number of Iterations	686	645	610	7	5	N.C.[f]	6	5	5	N.C.
Computing Time(sec)[g]	46.03	190.65	235.19	1.10	2.34	-	0.98	2.97	16.1	-

[a]: AADR(n) with the normal S_2-like weighting function ($W = |\mu| + |\eta| - 0.5$),
[b]: AADR(d) with the directional S_2-like weighting functions
($W_x = 0.6(|\mu| - |\eta|) + 1,\ W_y = -0.6(|\mu| - |\eta|) + 1$),
[c]: DANTSYS code system, [d]: Constant-constant nodal scheme,
[e]: Constant-linear nodal scheme, [f]: Not converged, [g]: SUN-ULTRA1.